# Vibration Control of Cable-Driven Parallel Robot for 3D Printing

Florian Lacaze, Simon Chesné, Didier Rémond

# Vibration Control of Cable-Driven Parallel Robot for 3D Printing

Florian LACAZE[1], Simon CHESNE[1], Didier REMOND[1]

[1]Univ Lyon, INSA-Lyon, CNRS UMR5259, LaMCoS, F-69621, France
florian.lacaze@insa-lyon.fr

## Abstract

These last years, the additive manufacturing and 3D printing technologies have known some major breakthroughs. The motion of a printer head can be made with cable transmission. The deployment of the cable-driven parallel robots (CDPR) in the industry is studied in very various application fields for their low cost and large workspace. Furthermore, the use of cables for the transmission induces a reduction of the mobile parts' masses, compared to a rigid transmission, which enables to reach higher accelerations. Moreover, the structure of a CDPR is modular and reconfigurable thanks to the repositioning of the actuators' anchor points. However, the lack of rigidity of a CDPR raises issues of accuracy and the rise of vibrations, which can be generated by the trajectory of the mobile parts, the actuators, the friction between pulleys and cables or disturbances.
Several dynamic models of cables have been studied to understand the vibrating behaviour of a CDPR: a simple elastic model of springs with positive tensions, a lumped mass-spring model and a finite elements model based on a continuous one for the cables dynamics. The numerical simulation of the dynamic behaviour of the CDPR with these models enables the analysis of an appropriate control system and the design of a controller. It aims at ensuring an accurate positioning and a decrease of vibrations.
In this contribution, we will firstly present the dynamic behaviour's model and the issue of the actuation's redundancy, systematically present on these robots to guarantee stiffness with the tension in the cables. A comparison will be done between the effects of the models on the conception and the performance of the controller. Thus, we explain that significant decreases in the vibration levels may be observed with the use of PID controllers. The generalisation of the command, the use of active control technologies and an experimental validation will be the next steps of this study.

## 1 Introduction

Cable-Driven Parallel Robots (CDPR) are a type of parallel kinematic machines in which cables link a mobile platform to a fixed base. Reels allow the control of cables length and cables tension. Several applications of CDPR have been studied, such as high speed manipulation [1], heavy materials handling [2], haptic perception [3]. Their large workspace enables to visualise [4, 5] or print [6] large 3D objects.

Modelling CDPR requires to take into account the cables dynamics, which are complex and non-linear. The main models of cables dynamics are the following :

- Elastic models (valid and efficient for low-density and thin cables);
- Analytic models with non-linear equations (Irvine model [7]);
- Semi-analytic methods for cable with small sag [8, 9];
- Lumped mass methods [10];
- Finite element models, using cables with time-dependent length [11, 12]

.

A CDPR constituted of a punctual mass linked by two cables driven by two actuators is considered in the following paper. It is an over-actuated CDPR, since the only controlled Degree Of Freedom (DOF) of the effector is the horizontal position.

The contribution of this paper is to compare three dynamic models of a CDPR in Section 2: an elastic spring model, a lumped mass-spring model and a variable length finite elements model. Section 3 is dedicated to the strategies of command. Results are discussed in Section 4.

# 2 Models of dynamic behaviour

## 2.1 Elastic model

An effector of mass $M$ is linked with two cables, modelled by two elastic springs. The cables tension is controlled by means of actuators, allowing the effector motion control. The distance between the two cable reels $A_1$ and $A_2$ is $d = 1$ m. This configuration is shown in Figure 1.

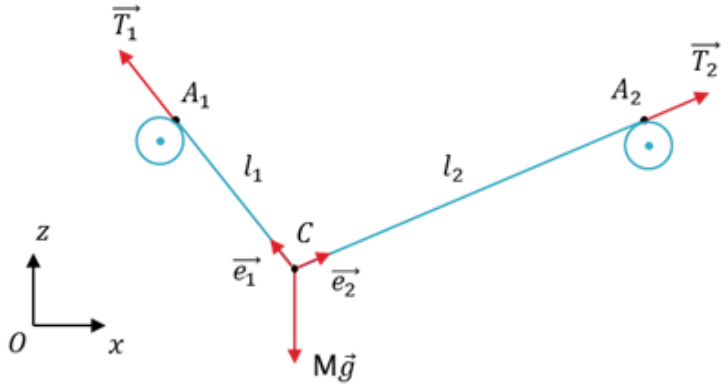


Figure 1: CDPR with 2 cables

Given the Young's modulus $E = 102$ GPa of the cable and its cross-sectional area $A = 1.76e^{-6}$ m$^2$, the cable tension can be described as :

$$T = EA\frac{l - l_0}{l_0} \tag{1}$$

with $l$ the strained cable length and $l_0$ the unstrained cable length.

The effector of mass $M$ is constrained under the two cable tensions $T_1$ and $T_2$, and its dynamic equation is given by :

$$\begin{pmatrix} \ddot{x} \\ \ddot{z} \end{pmatrix} = \frac{1}{M}(T_1\vec{e_1} + T_2\vec{e_2}) + \vec{g} \tag{2}$$

Unit vectors state the direction of efforts transmitted through the cables. For the $i^{th}$ cable, we have :

$$\vec{e_i} = \frac{\overrightarrow{OA_i} - \overrightarrow{OC}}{||\overrightarrow{OA_i} - \overrightarrow{OC}||} \tag{3}$$

## 2.2 Lumped mass-spring model

Each cable is now lumped into $N = 40$ mass-spring elements. Each of them is formed by a spring, of unstrained length $l_0 = \frac{L_0}{N}$ and stiffness $k_0 = \frac{EA}{l_0}$, and by a mass $m = \rho A l_0$.

As shown in Figure 2, the length of modelled cable is larger than the length between $A_1$ and the end-effector. The purpose is to have always the same amount of elements when the effector is moving. The cable located to the left of $A_1$ and to the right of $A_2$ corresponds to the cable rolled in the reels.

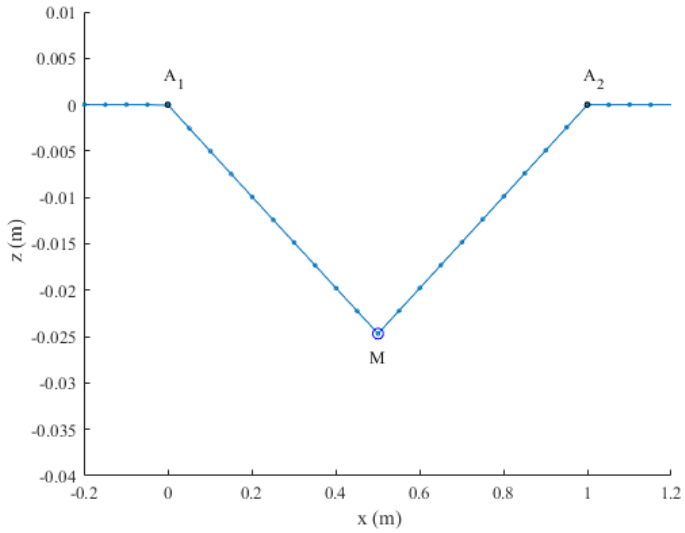


Figure 2: Lumped mass-spring model

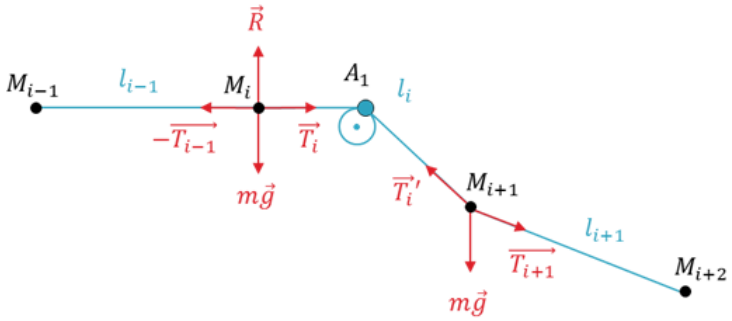


Figure 3: 3 elements of the lumped mass-spring model

To understand the difference of dynamics between the rolled cable and the free one, the Figure 3 gives a closer look at the lumped mass-spring model near $A_1$. We consider the points $M_j$ with $j = \{i-1, i, i+1, i+2\}$. The corresponding lengths are :

$$\begin{cases} l_{i-1} = ||\overrightarrow{M_{i-1}M_i}|| \\ l_i = ||\overrightarrow{M_iA_1}|| + ||\overrightarrow{A_1M_{i+1}}|| \\ l_{i+1} = ||\overrightarrow{M_{i+1}M_{i+2}}|| \end{cases} \tag{4}$$

The tensions, computed using these lengths, are the following :

$$\begin{cases} T_{i-1} = k(l_{i-1} - l_0) \\ T_i = k(l_i - l_0) \\ T_{i+1} = k(l_{i+1} - l_0) \end{cases} \tag{5}$$

We can also determine the accelerations $\ddot{X}_i = \begin{pmatrix} \ddot{x}_i \\ \ddot{z}_i \end{pmatrix}$ and $\ddot{X}_{i+1}$ before and after $A_1$. In $M_i$ the mass element is only constrained by horizontal tensions and in $M_{i+1}$ unit vectors give the directions of the efforts :

$$m\ddot{X}_i = \begin{pmatrix} -T_{i-1} + T_i \\ 0 \end{pmatrix} \tag{6}$$

$$m\ddot{X}_{i+1} = \begin{pmatrix} T_i \frac{x_{A_1} - x_{i+1}}{||\overrightarrow{A_1M_{i+1}}||} + T_{i+1}\frac{x_{i+2} - x_{i+1}}{l_{i+1}} \\ T_i \frac{z_{A_1} - z_{i+1}}{||\overrightarrow{A_1M_{i+1}}||} + T_{i+1}\frac{z_{i+2} - z_{i+1}}{l_{i+1}} \end{pmatrix} - m\vec{g} \tag{7}$$

### 2.3 Variable length finite elements model

We consider that each cable is divided in $N = 10$ elements with the same unstrained length $l = \frac{L}{N}$. The length $l$ is time-depending during the movement of the CDPR and its variations are taken into account in the dynamics. The details of the equations can be found in the article of J. Du and al. [13].

For a cable of length $l$, the kinetic energy is :

$$T = \int_0^l \frac{1}{2}\mu \dot{\vec{r}}^T . \dot{\vec{r}} \mathrm{d}s \tag{8}$$

where $\mu$ is the mass per unit length and $\vec{r}$ is the position vector of the element.

The elastic potential and gravitational potential energy of the same cable is :

$$U = \int_0^l (\frac{1}{2}EA\varepsilon^2 - \mu g \vec{r}^T . \vec{z})\mathrm{d}s \tag{9}$$

where $\varepsilon$ is the element strain.

The changing mass of the system can be written as :

$$\delta H = \delta \vec{r}_j{}^T f_j + \mu \dot{\vec{r}}_1{}^T . \delta \vec{r}_1 v_1 + \mu \dot{\vec{r}}_2{}^T . \delta \vec{r}_2 v_2 \tag{10}$$

with $v_1$ the winding speed in $A_1$ and $v_2$ the winding speed in $A_2$.

The application of the Hamilton's principle on the cables gives the following equation :

$$\int_0^t T\mathrm{d}t - \delta \int_0^t U\mathrm{d}t + \int_0^t \delta H \mathrm{d}t = 0 \tag{11}$$

Eventually, this leads to the dynamic equation, which describes the position $\vec{r}_j$ of the $j$ index point :

$$\mathbf{m_j}\ddot{\vec{r}}_j + \mathbf{c_j}\dot{\vec{r}}_j + \mathbf{k_j}\vec{r}_j = \vec{f}_j + \vec{f}_j^g \tag{12}$$

In Eq. 12, $\mathbf{m_j}$ is the conventional mass matrix, $\mathbf{c_j}$ describes, with convective terms, an energy transfer due to length variations. The stiffness matrix $\mathbf{k_j}$ is composed of the axial deformation of the element and of a second term due to the first and second derivatives of the element length variation with respect to time. $\vec{f}_j$ is the nodal force acting on the cable. $\vec{f}_g$ is the equivalent nodal force of the cable element self-weight.

## 3 Strategies of command

### 3.1 Trajectory

The chosen trajectory is a *step5*-function (Equation 13), which enables to avoid chocs and discontinuities and to lower vibrations. The principle is to go smoothly from $x_1$ to $x_2$ between $t_1$ and $t_2$ ; it means that the velocities at $t_1$ and $t_2$ are both equal to zero.

$$\mathrm{step5}(t) = \begin{cases} x_1 & \text{if } t < t_1 \\ x_1 + a\Delta^3(t)(10 - 15\Delta(t) + 6\Delta^2(t)) & \text{if } t_1 \leq t < t_2 \\ x_2 & \text{if } t \geq t_2 \end{cases} \tag{13}$$

with $a = x_2 - x_1$ and $\Delta(t) = \frac{t - t_1}{t_2 - t_1}$.

Here we consider $t_1 = 0$ s, $t_2 = 0.2$ s, $x_1 = 0.5$ m and $x_2 = 0.6$ m. The maximum speed in the case of the parameters mentioned below is $0.9375$ m.s$^{-1}$ at $t = 0.1$ s. The maximum acceleration is $\pm 14.434$ m.s$^{-2}$ at $t = (0.0423; 0.1577)$ s.

### 3.2 Control

There are two ways of controlling the end-effector of a CDPR : by controlling the cables length or their tension. The choice, here, has been made to control the cables tension, mainly for observed stability reasons. Moreover, the choice is led by the fact that the mechanism is redundantly constrained, which means that the number of cables driving the end-effector is one greater than the number of the robot's DOF.

Because of the actuation's redundancy, we face an issue of tension distribution in the cables. The next step is to chose a set of additional equality or inequality constraints before designing an algorithm of optimisation that finds an optimal tension distribution [14]. The most commonly used constraints in order to get the optimal tension distribution are :

- positive cables tension (to avoid an unstressed cable) [15];
- minimal sum of cables tension (to minimise the actuators' energy);
- tensions in an interval $[t_{min};t_{max}]$ [16];
- continuous cables tension.

For the tensions distribution, we chose to force 100 N of pretension on each cable, which means that $\sum T = T_1 + T_2 = 200$ N. PID controllers are robust enough to be used in CDPR control, even if CDPR behaviour is non-linear [17]. Our PID controller provides the effort needed by the effector so that it follows the desired trajectory. Thus, the tensions distribution in the controllers will be written : $T_1 = \frac{\sum T - F}{2}$ and $T_2 = \frac{\sum T + F}{2}$.

The controllers' gains have been settled on the elastic model, which enables a faster and easier setting. We do not present the optimisation of the parameters for the controller, but a comparison between the controlled models. The PID controllers' gains for each model are :

$$\begin{cases} P = 1860 \\ I = 8700 \\ D = 100 \\ \text{filter coefficient } N = 540 \end{cases}$$

The blocks containing the calculation of the trajectory, the controller and the dynamic model are shown in the Figure 4.

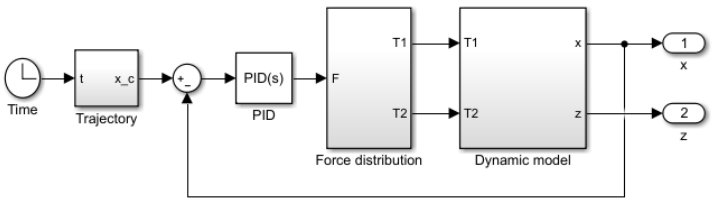


Figure 4: Simulink diagram

## 4 Results and discussion

Computation of the dynamic models is done using MATLAB and SIMULINK. Parameter settings of the numerical simulation are as follows : MATLAB solver used is *ode45*, the relative tolerance is $1e^{-5}$, the minimum time step is $1e^{-5}$ s and the sample time is $1e^{-}5$ s.

The initial position of the elastic model (Section 2.1) is computed by solving the static equilibrium of the Equation 14, which gives the starting position for the end-effector.

$$T_1\vec{e_1} + T_2\vec{e_2} + M\vec{g} = \vec{0} \tag{14}$$

To get the initial positions of the models presented in 2.2 and 2.3, we add a damping in the dynamic parameters of the model and we compute a free simulation in order to determine the equilibrium of each element of the model. The Figure 5 outlines the simulation results of the three dynamic models introduced in Section 2 for a computing time of $t_{\text{final}} = 5$ s. Very small oscillations, in the range of $1e^{-5}$ m, are observed for $x$. They are similar in all the models. The error, computed by $error = x_{\text{trajectory}} - x_{\text{effector}}$ and presented in Figure 6, is lower than $1e^{-2}$ in the transition phase, and lower than $1e^{-5}$ after 1 s of simulation.

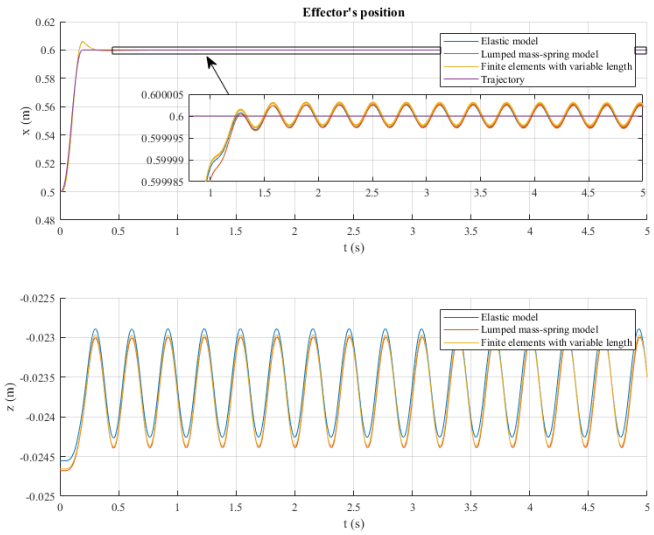


Figure 5: Evolution of $x$ and $z$ effector's position

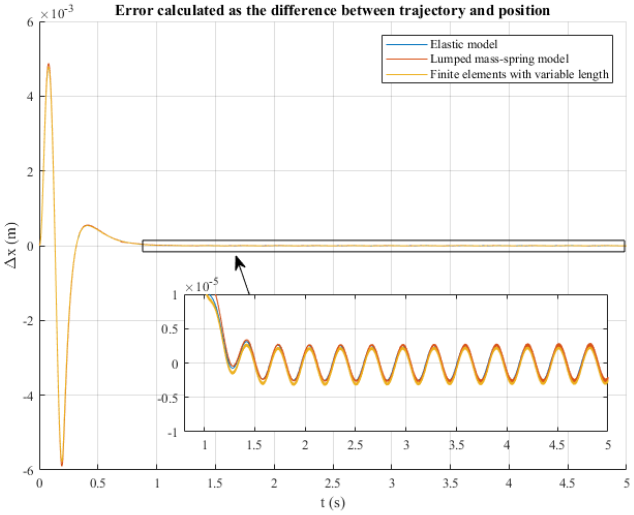


Figure 6: Position error of the CDPR

For $z$, oscillations are observed at the same frequency, with an amplitude of 1 mm. The mean of $z$ oscillations in the elastic model is higher than in the two other models, because this one does not take into account the mass of the cables. The Figure 7 shows a spectrum analysis of the error signals between $t = 1$ s and $t = 5$ s. A peak at 20.11 rad.s$^{-1}$ is observed for the three models. It corresponds to the end-effector's vertical oscillations,

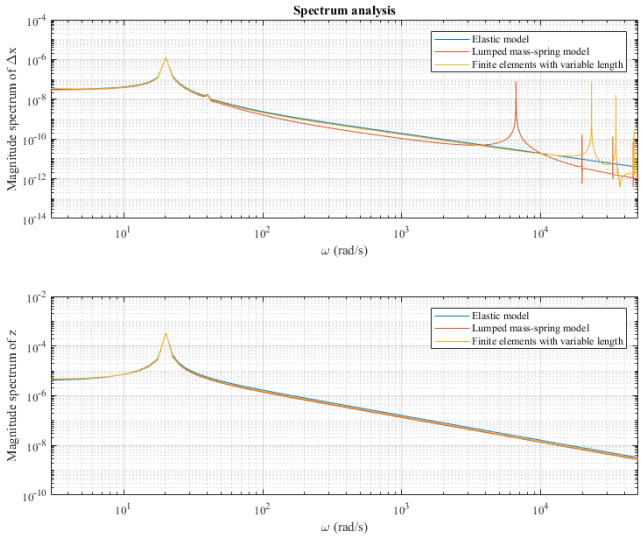


Figure 7: Spectrum analysis of $\Delta x$ and $z$

as shown in Figure 5. The vertical resonance frequency of a system constituted of two strings and one mass is given by the following equation :

$$\omega = \sqrt{\frac{T}{M}\left(\frac{1}{x} + \frac{1}{d-x}\right)} \tag{15}$$

With the parameters values used in the three models, this resonance frequency is equal to 20.41 rad.s$^{-1}$, which is closed to the frequency of the peak on the spectrum. The high frequency peaks, observed for the lumped mass-spring model and the variable length finite elements model, corresponds to the discretization of the cables.

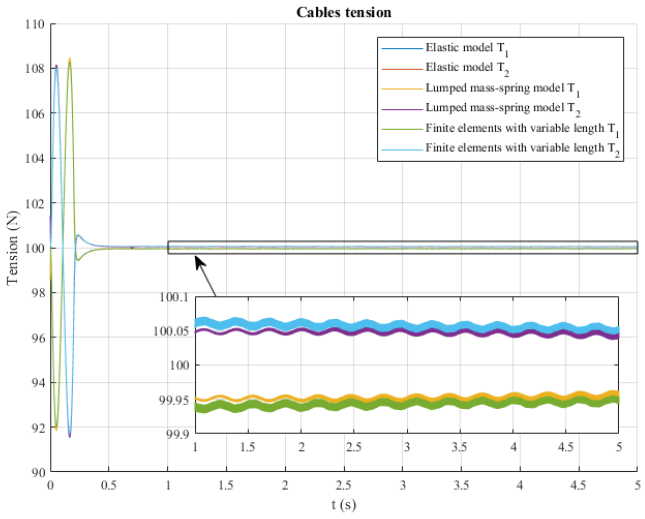


Figure 8: Cables tension $T_1$ and $T_2$

Figure 8 represents the evolution of the cables tension. In order to follow the trajectory acceleration, the tension $T_1$ decreases down to 92 N, then increases up to 108 N, and finally stabilises around 99.95 N. The tension $T_2$ does an inverse evolution and finally stabilises around 100.05 N. In the configuration where the effector's

position is $x = 0.6$ m, the two tensions are not exactly the same because the cables are not symmetrical. This enables the end-effector to get the desired position .

# 5 Conclusion

Three cable models for a CDPR have been presented in this paper : an elastic model, a lumped mass-spring model and a finite elements model. Eventually, these models' results are consistent with each others. For the three models, the PID controller enables to achieve good performances. Indeed, the static error is lower than $1e^{-5}$ and the overshoot is lower than 1 cm. It can be noticed that the PID controller is robust enough to control the effector's position and keeps constant gains, regardless of the dynamic model used in the simulation. The gains' adjustment was not problematic to control numerical models, thus we can hope that adjusting the gains on an experimental model will not be problematic either.

In further studies, we shall test other strategies of control, such as inverse dynamics control or model-free control, add the behaviour of the actuators to the dynamic model, and build a test bench to bring an experimental validation to the results that are introduced in this paper.

# References


[1] Sadao Kawamura, Hitoshi Kino, and Choe Won. High-speed manipulation by using parallel wire-driven robots. *Robotica*, 18(1):13–21, 2000.

[2] Roger Bostelman, James Albus, Nicholas Dagalakis, Adam Jacoff, and John Gross. Applications of the nist robocrane. In *Proceedings of the 5th International Symposium on Robotics and Manufacturing*, pages 14–18, 1994.

[3] Martin Otis. *Analyse, commande et intégration d'un mécanisme parallèle entraîné par des câbles pour la réalisation d'une interface haptique comme métaphore de navigation dans un environnement virtuel*. PhD thesis, Faculté des études supérieures de l'Université Laval, 2009.

[4] Clément Gosselin and Samuel Bouchard. A Gravity-Powered Mechanism for Extending the Workspace of a Cable-Driven Parallel Mechanism: Application to the Appearance Modelling of Objects. *International Journal of Automation Technology*, 4(4):372–379, July 2010.

[5] Samuel Bouchard. *Géométrie des Robots Parallèles Entraînés par des Câbles*. PhD thesis, Faculté des études supérieures de l'Université Laval, 2008.

[6] Eric Barnett and Clément Gosselin. Large-scale 3d printing with a cable-suspended robot. *Additive Manufacturing*, 7:27–44, July 2015.

[7] H. Max Irvine. *Cable structures*, volume 17. MIT press Cambridge, MA, 1981.

[8] Younes Achkire. *Active Tendon Control of Cable-Stayed Bridges*. PhD thesis, Université Libre de Bruxelles, 1997.

[9] Frederic Bossens. *Amortissement actif des structures câblées : de la théorie à l'implémentation*. PhD thesis, Université Libre de Bruxelles, 2001.

[10] Donya Mohammadshahi. *Dynamics and Control of Cables in Cable-Actuated Systems*. PhD thesis, McGill University, Montreal, 2013.

[11] Haluk Ozdemir. A finite element approach for cable problems. *International Journal of Solids and Structures*, 15(5):427–437, 1979.

[12] P.-H. Wang, R.-F. Fung, and M.-J. Lee. Finite Element Analysis of a Three-Dimensional Underwater Cable with Time-Dependent Length. *Journal of Sound and Vibration*, 209(2):223–249, January 1998.

[13] Jingli Du, Chuanzhen Cui, Hong Bao, and Yuanying Qiu. Dynamic Analysis of Cable-Driven Parallel Manipulators Using a Variable Length Finite Element. *Journal of Computational and Nonlinear Dynamics*, 10(1):011013, September 2014.

[14] G. Meunier, B. Boulet, and M. Nahon. Control of an Overactuated Cable-Driven Parallel Mechanism for a Radio Telescope Application. *IEEE Transactions on Control Systems Technology*, 17(5):1043–1054, September 2009.

[15] So-Ryeok Oh and S.K. Agrawal. Cable-suspended planar parallel robots with redundant cables: controllers with positive cable tensions. In *2003 IEEE International Conference on Robotics and Automation (Cat. No.03CH37422)*, volume 3, pages 3023–3028, Taipei, Taiwan, 2003. IEEE.

[16] Johann Lamaury. *Contribution à la commande des robots parallèles à câbles à redondance d'actionnement*. PhD thesis, Université Montpellier II - Sciences et Techniques du Languedoc, 2014.

[17] A. Mohammad Khosravi and Hamid D. Taghirad. Robust PID control of fully-constrained cable driven parallel robots.